Available online at www.sciencedirect.com
ScienceDirect
Journal of the European Ceramic Society 27 (2007) 2995–2999
www.elsevier.com/locate/jeurceramsoc

Extended X-ray absorption fine structure, X-ray diffraction and Raman analysis of nickel-doped $Ba(Mg_{1/3}Ta_{2/3})O_3$

Mei Yu Chen [a], P.J. Chang [a], C.T. Chia [a,*], Y.C. Lee [b], I.N. Lin [c], L.-J. Lin [d], J.F. Lee [e], H.Y. Lee [e], T. Shimada [f]

[a] *Department of Physics, National Taiwan Normal University, Taipei 116, Taiwan, ROC*
[b] *Department of Materials Science and Engineering, National Tsing-Hua University, 300 Taiwan, ROC*
[c] *Department of Physics, Tamkang University, Tamsui Taipei 251, Taiwan, ROC*
[d] *Material and Chemical Research Laboratories, Industrial Technology Research Institute, Chutung, Hsinchu 310, Taiwan, ROC*
[e] *National Synchrotron Radiation Research Center, Hsinchu 300, Taiwan, ROC*
[f] *R&D Center, NEOMAX Co. Ltd., 2-15-17 Egawa, Shimamoto, Osaka 618-0013, Japan*

Available online 11 December 2006

Abstract

Raman, X-ray diffraction and extended X-ray absorption fine structure (EXAFS) measurements of $x Ba(Ni_{1/3}Ta_{2/3})O_3 + (1-x)Ba(Mg_{1/3}Ta_{2/3})O_3$ samples with $x = 0$–0.03 were performed to reveal the nickel doping effect on the microwave properties. EXAFS result clearly shows that the nickel is located on the Mg lattice site. We also found that, as the nickel concentration increases, microwave dielectric constant decreases with the Ta–O and Ni–O bond distances. X-ray diffraction shows that the 1:2 ordered structure is degraded with the increasing of nickel concentration. The stretching phonon of the TaO_6 octahedra, that is $A_{1g}(O)$ phonon near 800 cm^{-1}, are strongly correlated to the microwave properties of $x Ba(Ni_{1/3}Mg_{2/3})O_3 + (1-x)Ba(Mg_{1/3}Ta_{2/3})O_3$ samples. The large Raman shift and the large width of the $A_{1g}(O)$ imply rigid but distorted oxygen octahedral structure, therefore, the effect of nickel doping lowers the dielectric constant and the $Q \times f$ value of $Ba(Mg_{1/3}Ta_{2/3})O_3$ ceramic.

Keywords: Extended X-ray absorption fine structure (EXAFS)

1. Introduction

$Ba(Mg_{1/3}Ta_{2/3})O_3$ perovskite ceramic is known for its low dielectric loss and high $Q \times f$ value in microwave region.[1] However, the high cost of Ta_2O_5 powder and the high sintering temperature (above 1600 °C) of $Ba(Mg_{1/3}Ta_{2/3})O_3$ raise the cost price for the industrial application.[2] Nomura et al.[1,3] found the doping of BMT with 1 mol% of Mn not only promotes sinterability by lowering the sintering temperature but also increases the $Q \times f$ value appreciably. Matsumoto et al.[4] investigated the SnO_2-doped $Ba(Mg_{1/3}Ta_{2/3})O_3$ which had better microwave dielectric properties. The internal process and physics in $Ba(Mg_{1/3}Ta_{2/3})O_3$ with small amount of dopants are still under investigation. Surendran et al.[5] sums up the dopant effect on dielectric properties of $Ba(Mg_{1/3}Ta_{2/3})O_3$, and found that the valence charges and ionic radii of dopants affected the microwave dielectric properties of $Ba(Mg_{1/3}Ta_{2/3})O_3$ in a very different way.[5] Kim and Yoon[6] were the first group to investigate the nickel effect on the microwave dielectric properties of $Ba(Mg_{1/3}Ta_{2/3})O_3$. The results of scanning electron microscope and energy dissipation spectrum have shown that the grain size decreases with nickel doping concentration, therefore, the decrease of microwave dielectric properties may be attributed to the lower density and smaller grain size. Raman scattering is an excellent tools to investigate the phonon properties of 1:2 ordered perovskite materials, and researchers have found the correlation of phonon modes with the microwave properties.[7,8] A recent study has shown that stretching vibration of oxygen octahedral network and 1:2 ordered phonons of 1:2 ordered structure play an important role on the material microwave performance.[8] However, the Raman measurements yield information that indirectly relate phonon vibrations to the microwave properties. On the other hand, extend X-ray absorption fine structure (EXAFS) can probe $B''O_6$ local structure directly, and the structural properties of oxygen octahedra can be deduced and correlated to the microwave dielectric properties.[9]

* Corresponding author. Tel.: +886 2 29346620x141; fax: +886 2 29326408.
E-mail address: chiact@phy.ntnu.edu.tw (C.T. Chia).

0955-2219/$ – see front matter © 2006 Elsevier Ltd. All rights reserved.
doi:10.1016/j.jeurceramsoc.2006.11.025

X-ray diffraction method is also a useful tool to reveal the quality of 1:2 ordered structure of $Ba(Mg_{1/3}Ta_{2/3})O_3$. In this paper, we investigate the effect of small amount of nickel doping on the structural and microwave properties of $Ba(Mg_{1/3}Ta_{2/3})O_3$ by the Raman scattering, EXAFS and X-ray diffraction methods.

2. Experiment

The conventional mixed oxide process was adopted to prepare xBa$(Ni_{1/3}Ta_{2/3})O_3 + (1-x)Ba(Mg_{1/3}Ta_{2/3})O_3$ perovskite ceramic samples (hereafter xBNT + $(1-x)$BMT), while $x = 0.005$, 0.01, 0.015, 0.02, 0.025 and 0.03. The samples were sintered at 1600 °C with oxygen concentration over than 80%, and the sintering time was 25 h. The Raman measurements were performed at room temperature and signals were recorded by a DILOR XY-800 triple-grating Raman spectrometer equipped with a liquid-nitrogen-cooled CCD. The 10 mW output of the 514.5-nm line of Ar^+ ion laser was used as the excitation source. The obtained Raman spectra exhibited a resolution of 0.5 cm^{-1} approximately. The dielectric properties were measured by the TE011 resonant cavity method using an HP 8722 network analyzer at a frequency near 6 GHz.[10,11] X-ray diffraction results were analyzed by GSAS program[12,13] to deduce the ordering parameter of 1:2 order structures. The EXAFS data of Ni K-edge and Ta L_{III}-edge were measured at Wiggler beamline BL17C of National Synchrotron Radiation Research Center and analyzed by FEFF-8 program.[14–21] The intensity of the incidence X-ray was monitored by the ionization chamber and the obtained absorption signal raised at the absorption edge was used to deduce the concentration of the absorbing atoms.[20] In the following, the results of Raman, X-ray diffraction and EXAFS revealed structural factors that directly affect the microwave performance are discussed.

3. Result and discussion

Fig. 1 shows the Raman spectra of xBNT + $(1-x)$BMT accompanied by an intense background which decreases with the Ni doping concentration. Four dominant Raman peaks can be clearly found, and they are $A_{1g}(Ba) + E_g(Ba)$ near 105 cm^{-1}, $E_g(O)$ around 375 cm^{-1}, $E_g(O)$ at 431 cm^{-1} and the stretching vibrations of TaO_6 $A_{1g}(O)$ near 800 cm^{-1}.[8] Beside these four dominant modes, three weak phonons in between 150 and 300 cm^{-1} are observed. In Fig. 2(a), the Raman shift of stretching mode, $A_{1g}(O)$, of TaO_6 and the dielectric constant are plotted as a function of nickel concentration. As the nickel concentration increases, the dielectric constant drops, while the Raman shift of $A_{1g}(O)$ increases. The Raman shift of the stretching $A_{1g}(O)$ phonon is related to the Ta–O bond strength, hence the lager Raman shift indicates the rigid TaO_6 octahedral structure, hence a larger Raman shift indicates a more rigid octahedron lowers the dielectric constant. Similarly, the width of $A_{1g}(O)$ mode and $Q \times f$ value as function of Ni concentration are plotted in Fig. 2(b). The width of stretching $A_{1g}(O)$ phonon of octahedron increases with Ni concentration, while the $Q \times f$ value decrease with doping concentration. The phonon width is related to the lifetime of the phonon propagation, and larger widths give short

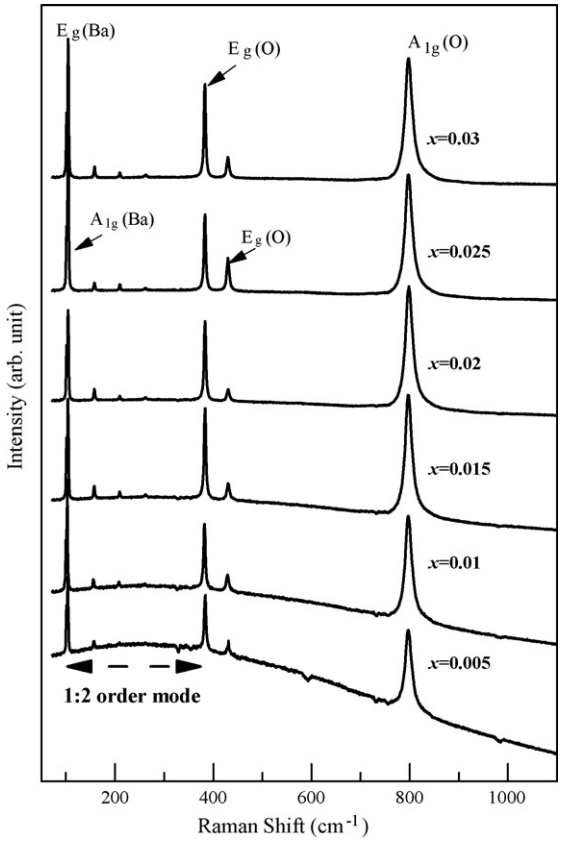

Fig. 1. Raman spectra of xBNT + $(1-x)$BMT samples with $x = 0.005$–0.03.

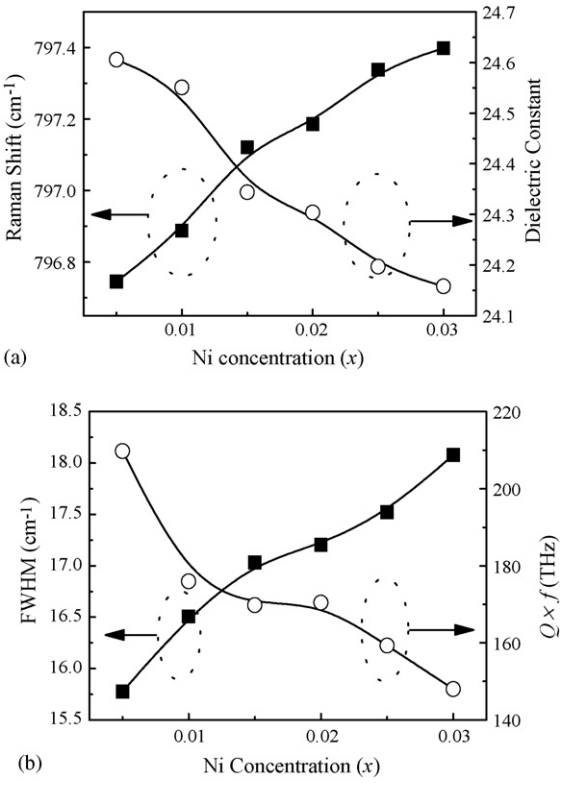

Fig. 2. Correlation of $A_{1g}(O)$ phonon characteristics with the microwave properties of xBNT + $(1-x)$BMT: (a) the correlation of Raman shift and the dielectric constant and (b) FWHM and the $Q \times f$ value.

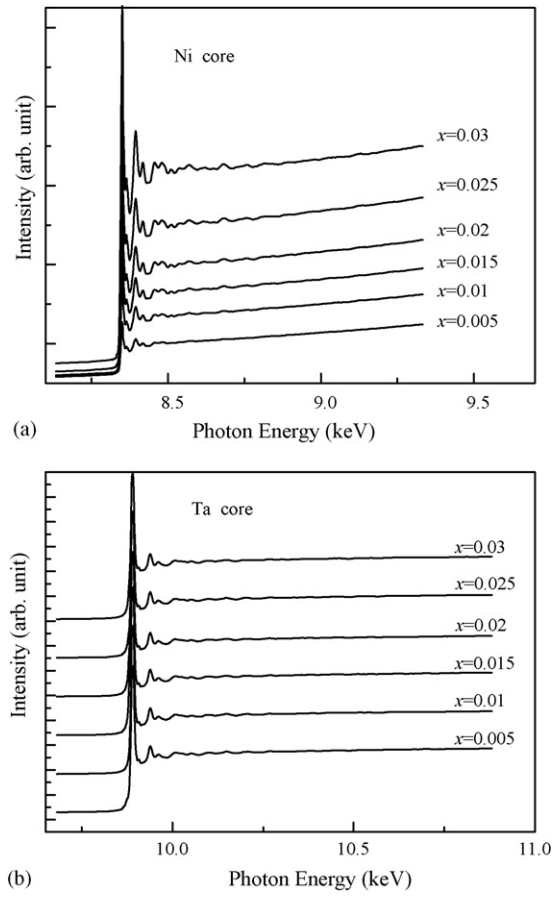

Fig. 3. (a) Ta L_{III}-edge and (b) Ni K-edge EXAFS spectra of xBNT + $(1-x)$BMT.

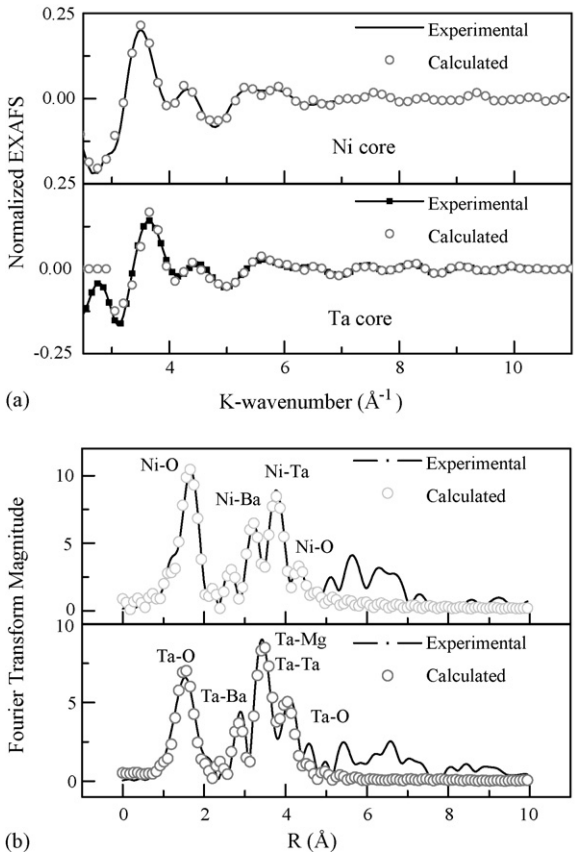

Fig. 4. The EXAFS signal of 0.005BNT + 0.995BMT: (a) momentum (k^3) weighted EXAFS signal of Ta L_{III}-edge and Ni K-edge in momentum space, and (b) in R space. The solid lines represent the experiment data, while the hollow circles are FEFF-8 fitting results.

lifetimes due to poor crystalline. The microwave $Q \times f$ value is also related to the propagation length of the microwave. Raman result indicates that the structural properties of oxygen octahedra do have effect on the microwave $Q \times f$, as we found in Fig. 2(b). However, it is very hard to resolve the structural parameter from Raman measurement.

The EXAFS measurement of xBNT + $(1-x)$BMT are showed in Fig. 3, in order to resolve the structure of the TaO_6 and NiO_6. The X-ray absorption coefficient of Ni rised at K-edge near 8333 eV are shown in Fig. 3(a), is proportional to the Ni concentration as expected. Fig. 3(b) shows the EXASF of Ta absorption coefficient at L_{III}-edge around 9881 eV. By using AUTOBK program to remove the backgrounds of the curves shown in Fig. 3, the interference oscillation which is caused by backscattering of surrounding atoms of Ni or Ta can be obtained. Fig. 4(a) shows the k-weighted $[k^3\chi(k)]$ EXAFS signals at the range 3–12 $Å^{-1}$ in k space. Fig. 4(b) shows the Fourier transformation of the k-weighted $[k^3\chi(k)]$ EXAFS signals of Ta and Ni core atoms, and these two curves are obviously different. This is the direct evidence that Ni atoms sit at Mg lattice sites. To deduce the structural parameters of the NiO_6 and TaO_6, backscattering interference functions from 0.9 to 4.2 Å were calculated by using the FEFF-8.2 program. In Fig. 4, the solid lines are experimental data, and the hollow lines are fitting curves. The R-factors of fitting are all below 0.03. Fig. 5 shows the average bond distance of Ni–O and Ta–O cores and the dielectric constant versus Ni concentration. Apparently, the size of the NiO_6 and TaO_6 octahedra, decrease with the Ni concentration, and this is consistent with the Raman results. When the average sizes of oxygen octahedra drop, the oxygen octahedra become more rigid. The displacement of B″ site atom caused by the applied external microwave is smaller in rigid oxygen octahedra and lower dielectric constants are expected.

Fig. 6 shows the XRD pattern of xBNT + $(1-x)$BMT samples. All the peaks were indexed to the 1:2 ordered hexagonal

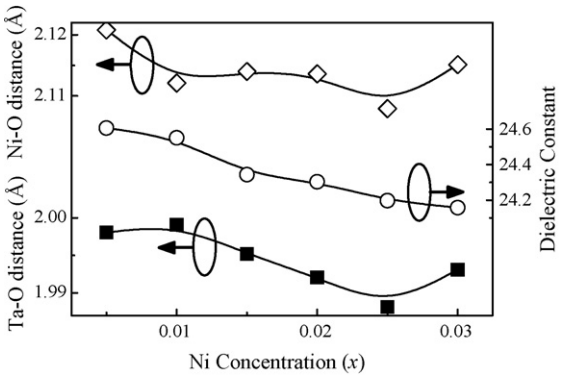

Fig. 5. Plot of the Ni–O and Ta–O bond lengths and dielectric constants of xBNT + $(1-x)$BMT ceramics against of Ni concentration.

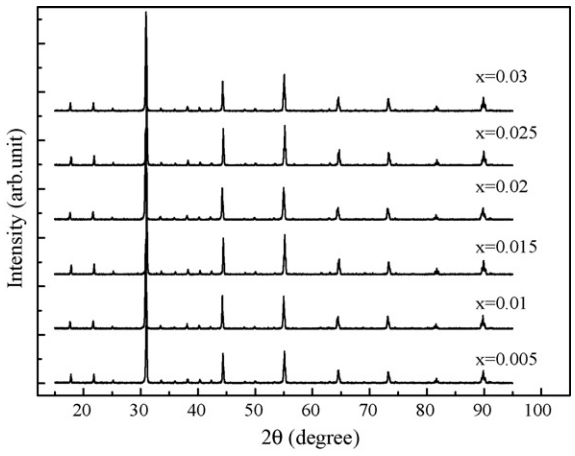

Fig. 6. The XRD patterns of xBNT + $(1-x)$BMT with $x = 0.005$, 0.01, 0.015, 0.02, 0.025 and 0.03.

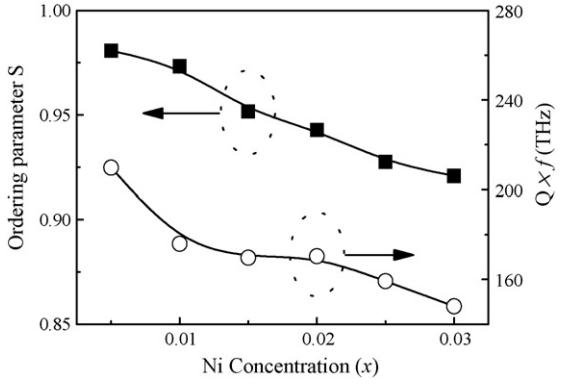

Fig. 7. The plot of the ordering parameters and $Q \times f$ values of xBNT + $(1-x)$BMT vs. Ni concentration.

unit cell. The peaks for the second phase were not observed. The crystal parameters and long-range-order parameter were obtained by Rietveld method. The long-range-order parameter, S, of xBNT + $(1-x)$BMT which is calculated from both the occupancy of Mg ions at Mg-site (ρ_{Mg}) or Ta ion at Ta-site (ρ_{Ta}),[22–23] that is:

$$S = \frac{\rho_{Mg} - (1/3)}{1 - (1/3)} = \frac{\rho_{Ta} - (2/3)}{1 - (2/3)}.$$

The long-range-order parameter represents the degree of the 1:2 ordered structure, and it is directly correlated to the $Q \times f$ value. As shown in Fig. 7, the higher long-range-order parameter is the higher the $Q \times f$ values are. This result indicates the 1:2 ordered structures are degraded by the Ni substitution.

4. Conclusion

The characteristics of oxygen octahedron play an important role for the microwave dielectric properties. The Raman result show the strongly correlation between stretching vibration of TaO_6 octahedron (i.e. A_{1g}(O) mode) and microwave dielectric properties. Large Raman shift leads to small dielectric constant, while broad width of A_{1g}(O) mode indicates low $Q \times f$ value. In the other words, this result indicates a rigid oxygen cage results in the small dielectric constant and high $Q \times f$ value. The EXAFS result shows that Ni sits on the Mg lattice site, and that smaller volumes of oxygen cage give small dielectric constant. The XRD result shows that no second phase occurs, but the 1:2 ordering structure is degraded by Ni substitution. The long-range-order parameter closely correlates with $Q \times f$ value, and indicates the $Q \times f$ value is dominated by 1:2 order structures.

Acknowledgements

Financial support of this work from the National Science Council of Taiwan, ROC, under the Contract Nos. NSC 94-2112-M-003-007 and NSC 93-2112-M-003-012 is acknowledged.

References

1. Nomura, S., Toyama, K. and Kaneta, K., $Ba(Mg_{1/3}Ta_{2/3})O_3$ ceramics with temperature-stable high dielectric constant and low microwave loss. *Jpn. J. Appl. Phys.*, 1982, **21**, L624–L626.
2. Katayama, S., Yoshinaga, I., Yamada, N. and Nagai, T., Low-temperature synthesis of Ba $(Mg_{1/3}Ta_{2/3})O_3$ ceramics from Ba–Mg–Ta alkoxide precursor. *J. Am. Ceram. Soc.*, 1996, **79**, 2059–2064.
3. Nomura, S., Ceramics for microwave dielectric resonator. *Ferroelectrics*, 1983, **49**, 61–70.
4. Matsumoto, H., Tamura, H. and Wakino, K., Ba(Mg, Ta)O_3-$BaSnO_3$ high-Q dielectric resonator. *Jpn. J. Appl. Phys.*, 1991, **30**(Part 1), 2347–2349.
5. Surendran, K. P., Sebastian, M. T., Mohanan, P. and Jacob, M. V., The effect of dopants in the microwave dielectric properties of $Ba(Mg_{1/3}Ta_{2/3})O_3$ ceramics. *J. Appl. Phys.*, 2005, **98**, 094114.
6. Kim, E. S. and Yoon, K. H., Effect of nickel on microwave dielectric properties of $Ba(Mg_{1/3}Ta_{2/3})O_3$. *J. Mater. Sci.*, 1994, **29**, 830–834.
7. Siny, I. G. and Katiyar, R. S., Cation arrangement in the complex perovskites and vibration spectra. *J. Raman Spectrosc.*, 1998, **29**, 385–390.
8. Chia, C.-T., Chen, Y.-C. and Cheng, H.-F., Correlation of microwave dielectric properties and normal vibration modes of $x Ba(Mg_{1/3}Ta_{2/3})O_3 - (1-x)Ba(Mg_{1/3}Nb_{2/3})O_3$ ceramics. I. Raman spectroscopy. *J. Appl. Phys.*, 2003, **94**, 3360–3364.
9. Chang, P. J., Chia, C.-T., Lin, I.-N., Lee, J. F., Lin, C.-M. and Wu, K. T., Characterizing $x Ba(Mg_{1/3}Ta_{2/3})O_3 + (1-x)Ba(Mg_{1/3}Nb_{2/3})O_3$ microwave ceramics using extended x-ray absorption fine structure method. *Appl. Phys. Lett.*, 2006, **88**, 242937.
10. Chen, M.-Y., Chia, C.-T., Lin, I.-N., Lin, L.-J., Ahn, C.-W. and Nahm, S., Microwave properties of $Ba(Mg_{1/3}Ta_{2/3})O_3$, $Ba(Mg_{1/3}Nb_{2/3})O_3$ and $Ba(Co_{1/3}Nb_{2/3})O_3$ ceramics revealed by Raman scattering. *J. Eur. Ceram. Soc.*, 2006, **26**(10–11), 1965–1968.
11. Kajfez, D. and Guillon, P., *Dielectric Resonators*. Artech House, Norwood, MA, 1986, pp. 65–111.
12. Rietveld, H. M., A profile refinement method for nuclear and magnetic structures. *J. Appl. Cryst.*, 1969, **2**, 65–71.
13. Larson, A. C. and Von Dreele, R. B., *GSAS-General Structure Analysis System*. Los Alamos National Laboratory, Los Alamos, New Mexico, 1994, pp. 86–748 [LAUR].
14. Koningsberger, D. C., and Prins, R. *X-ray Absorption Principles, Applications, Techniques of EXAFS, SEXAFS and XANES*, A Wiley-Interscience Publication.
15. Lipkin and Harry, J., Phase uncertainty and loss of interference in a simple model for mesoscopic Aharonov-Bohm experiments. *Phys. Rev. A*, 1990, **42**, 49–54.
16. Stern, E. A., Theory of the extended X-ray-absorption fine structure. *Phys. Rev. B*, 1974, **10**, 3027.
17. Newville, M., Ravel, B., Haskel, D., Rehr, J. J., Stern, E. A. and Yacoby, Y., Analysis of multiple-scattering XAFS data using theoretical standards. *Physica B*, 1995, **208–209**, 154–156.
18. Ravel, B., Practical introduction to multiple scattering theory. *J. Alloys Compd.*, 2005, **401**, 118–126.

19. Pfalzer, P. and Urbach, J. P., Elimination of self-absorption in fluorescence hard-X-ray absorption spectra. *Phys. Rev. B*, 1999, **60**, 9335–9339.
20. Wende, H., Recent advances in x-ray absorption spectroscopy. *Rep. Prog. Phys.*, 2004, **67**, 2105–2181.
21. Azaroff and Leonid, V., Theory of extended fine structure of X-ray absorption edges. *Rev. Mod. Phys.*, 1963, **35**, 1012–1021.
22. Moreira, R. L., Matinaga, F. M. and Dias, A., Raman-spectroscopic evaluation of the long-range order in $Ba(B_{1/3}'B_{2/3}'')O_3$ ceramics. *Appl. Phys. Lett.*, 2001, **78**, 428–430.
23. Cullity, B. D., *Element of X-ray Diffraction* (*2nd ed.*). Addison-Wesley, 1978, pp. 139, 328, 520, and 524.